ORIGINAL ARTICLE

Design of reinforced concrete structures from three-dimensional stress fields

Dimensionamento de estruturas de concreto armado a partir de campos de tensão tridimensionais

Reinaldo Chen[a]

Túlio Nogueira Bittencourt[a]

João Carlos Della Bella[a]

[a]Universidade de São Paulo – USP, Escola Politécnica, Departamento de Engenharia de Estruturas e Geotécnica, São Paulo, SP, Brasil

Abstract: The design of reinforced concrete structures starting from a linear analysis is allowed by design codes and leads to safe solutions. The structural model built for the analysis may be composed not only of bar and shell elements, but also solid elements. In the present work, the formulation of the Reinforced Solid Method (RSM) was reviewed and applied to the Ultimate Limit State design of a reinforced concrete member, with the computation of the required reinforcement and concrete check of each individual solid element within the structural model. The results were visualized in a post-processor and validated by numerical simulations. The RSM effectively allows for the design of concrete structures with general geometry and loading conditions, whilst identifying local effects throughout the volume of the structure.

Keywords: solid elements, reinforced concrete, design, reinforced solid method, three-dimensional elasticity.

Resumo: O dimensionamento de estruturas de concreto armado a partir de esforços provenientes de análise linear é permitido pelas normas e conduz a estruturas seguras. O modelo estrutural elaborado para a análise pode ser composto não somente de elementos de barra e de casca, mas também de elementos sólidos. Neste trabalho, a formulação do Método dos Sólidos Armados (MSA) foi revista e a aplicada ao dimensionamento em ELU de uma peça de concreto, com cálculo da armadura e verificação do concreto em cada um dos elementos sólidos componentes do modelo estrutural. Os resultados foram visualizados em um pós-processador e validados por simulações numéricas. O MSA permite o dimensionamento de estruturas com geometria e carregamento genéricos, identificando, ao mesmo tempo, efeitos localizados no interior do volume da estrutura.

Palavras-chave: elementos sólidos, concreto armado, dimensionamento, método dos elementos armados, elasticidade tridimensional.

1 INTRODUCTION

A concrete structure may be idealized from the composition of linear (bars), shell (membranes, plates, and shells), and solid elements. The utilization of finite solid elements may be justified when designing structural members with complex geometry and loadings, for which the application of unidimensional or bidimensional elements turns out to be insufficient to capture the load paths within the structure, such as those comprising industrial or hydraulic facilities (Figure 1). A linear analysis may be performed to determine the internal stress distribution throughout the three-dimensional structure for the ultimate limit state design, according to design codes [3]–[5]. The stress fields obtained

from the analysis consists of six stress components at each integration point of the solid elements comprising the structural model. Limiting state conditions are not directly expressed in terms of sectional forces, and the problem of dimensioning the required reinforcement and checking concrete in the presence of the applied stresses is then posed.
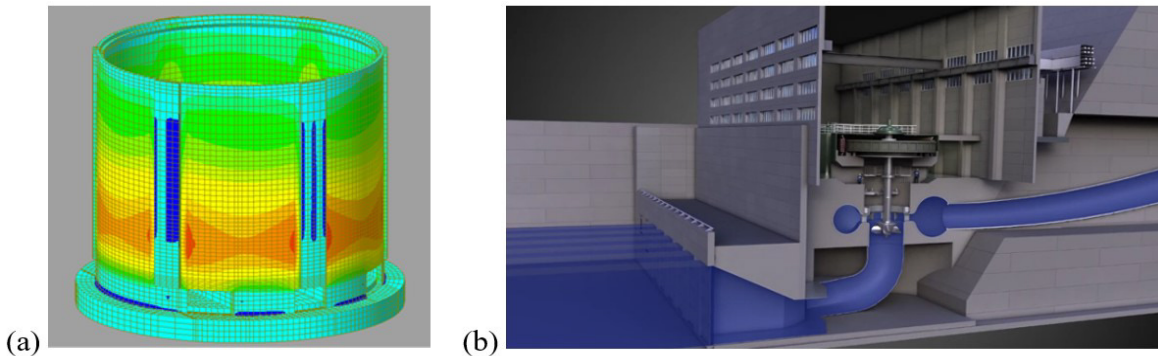
Figure 1. (a) Finite solid element model for a clinker storage silo of the Ramliya Cement Plant (Dianafea [1]); (b) concrete hydroelectric structure (Wikimedia Commons [2])

A solution for the design would be to provide reinforcement to resist the major principal stress in the principal directions. However, in design practice it is impossible to provide reinforcement following the randomly oriented principal tensile stresses within the structure, even more considering that a structural member is designed for multiple loading conditions. Alternatively, reinforcement could be arranged in three orthogonal directions to resist the major principal tensile stress in the three reinforcement directions. But this solution is also disregarded in design practice since uneconomical layouts would be attained, especially when crack directions draw close to any of the reinforcement directions. In another attempt, designers previously utilized the incomplete method of defining working sections and integrating the normal stress patterns over their surfaces and then calculating the reinforcement from the total sectional forces. For example, Boer [6] proposed the so-called "Theory on composing results to lower model type results" where one should proceed to the back-substitution of stresses from a solid model to reference elements: either by integration of stress components along the height of a structure to a bidimensional model at the level of a reference plane (Figure 2a), or by integration of stresses along both height and width of an elected cross-section to a unidimensional model at the level of a reference line (Figure 2b). Dolgikh and Podvysotskii [7] proposed, independently, the "Method of equivalent shells", which consisted basically in the same procedure as the one proposed by Boer, and applied it to the design of a concrete spillway (Figure 3). The method of composing results in reference elements, however, has restrict application to members with uniform geometry and loadings, so that a sectional design may effectively be performed. It cannot be applied in discontinuity regions such as joints of frames or zones of application of concentrated loads. As pointed out by Lisichkin [8], the results obtained by integration methods are "not rigorous since they did not incorporate either the tangential stresses or the effects of the resistance in the reinforcement to shearing in other directions."
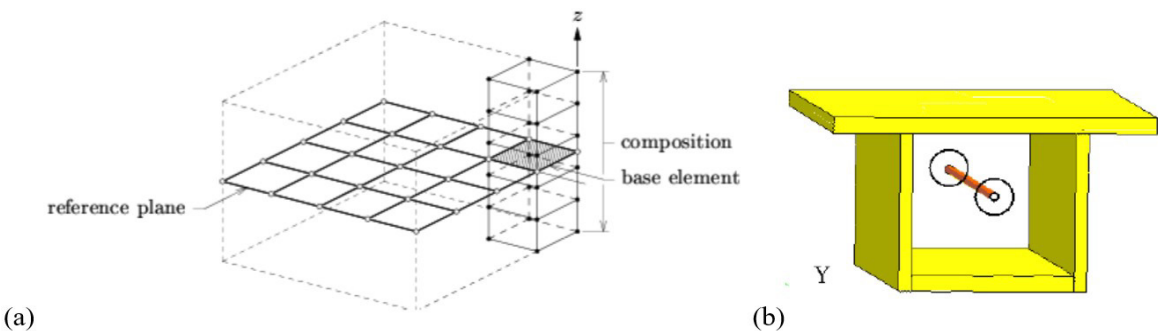
Figure 2. Composition of results from solid elements: (a) in a quadrangular reference plane or (b) in a reference line [6]
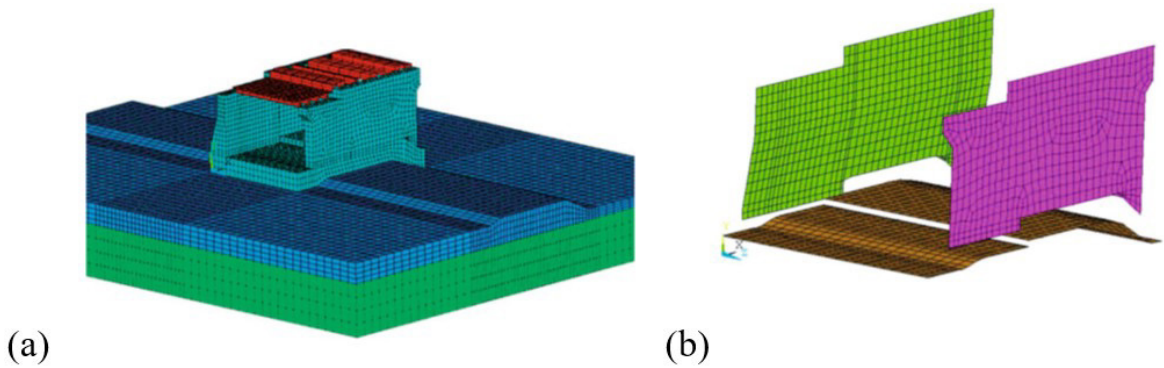
Figure 3. Finite element model for a concrete spillway: (a) with solid elements; (b) with equivalent shell elements
(Dolgikh and Podvysotskii [7])

The solution for the Ultimate Limit State (ULS) then relied on the definition of a resistant mechanism equilibrating the applied stress tensors. Smirnov [9], addressed, for the first time, equations for the reinforcement design in concrete solid elements from three-dimensional stress tensors, focusing on the application in hydroelectric structures. Kamezawa et al. [10] proposed additional formulas for the computation of the required reinforcement, but these were still limited to stress combinations yielding reinforcement in three directions. Marti, Mojsilović and Foster published two thorough detailed works on the subject [11], [12], clearly identifying biaxial and uniaxial compression design cases, and representing graphically the solution with the aid of Mohr circles. Their formulation was later reproduced in the *fib* Bulletin [13], which was a practical guide to finite element modelling of reinforced concrete structures. In this publication, however, no new information about the subject were brought. Hoogenboom and Boer [14], [15] categorized the solution into three subgroups, namely "corner", "edge" and "interior solution", according to the requirement of reinforcement in one, two or three orthogonal directions, respectively. They also implemented this solution in a numerical algorithm searching for the solution that minimized the total required steel. Su et al. [16] presented a genetic algorithm to examine all possible solutions and to find, among then, the one that provided the optimal reinforcement. Zalesov et al. [17] and Lisichkin [8] treated the theme with a different approach, where reinforcement incorporated shearing resistance. Since the solution was not analytical, but rather based upon coefficients determined experimentally, the derived equations are not presented in this work. Finally, Nielsen and Hoang presented the complete formulation in the third edition of the book *Limit Analysis and Concrete Plasticity* [18]. Former editions, dated of 1984 and 1999, still did not address this theme. The authors brought out the physical interpretation of the applied shear stresses and elegantly deducted analytically the complete set of design formulas of the reinforced solid method (RSM).

2 THE REINFORCED SOLID METHOD

The reinforced solid method (RSM) for the design of reinforced concrete structures combines linear stress analysis with limit design. A plastic method is in fact applied, and the lower bound theorem is recalled twice: first in the selection of a linear elastic statically admissible stress field equilibrating the design load (at the level of the global structure), and then in the calculation of the equivalent stresses on reinforcement and concrete composing a system of resistance that is statically able to carry the applied stresses, where the yield stress is nowhere violated (at the level of each individual element comprising the structure). The design load will be a safe estimate of the ultimate load of the structural member.

2.1. Application of limit analysis to structural concrete

Limit analysis was formulated for rigid-plastic materials and deals with the collapse load or the load-carrying capacity of a body at the yield point. The lower-bound theorem of limit analysis states that:

"Any load corresponding to a statically admissible state of stress (a state of stress that satisfies the equilibrium conditions and the statical boundary conditions for the actual load) everywhere at or below yield is not higher than the ultimate load."

A state of stress obtained from a linear elastic analysis represents a statically admissible stress field since equilibrium and static boundary conditions are satisfied. Concepts of limit analysis and their application to reinforced concrete were carefully reviewed and organized by several researchers [18]–[21]. Muttoni et al. [19] detailed the lower bound theorem for the application in reinforced concrete enunciating:

"In a plastic design a stress field is chosen such that the equilibrium conditions and the statical boundary conditions are fulfilled. The dimensions of cross-section and the reinforcement have to be proportioned such that the resistances are everywhere greater than or equal to the corresponding internal forces."

Kaufmann and Mata-Falcón [22] refer to Nielsen, Thürlimann and his coworkers as the pioneers in applying the theory of plasticity to reinforced concrete back to the second half of the last century, stating that "they were of course fully aware of the limited ductility of concrete and even reinforcement. Therefore, they completely neglected the tensile strength of concrete and addressed further concerns regarding ductility by providing minimum reinforcement and using conservative limits of the so-called effective concrete compressive strength as well as upper limits for the reinforcement quantities and corresponding compression zone depths (to avoid brittle failures due to concrete crushing)." Since then, design methods for three-dimensional structures based on the limit analysis have been developed, including the strut-and-tie method (STM) and the stress field method (SFM), (extensively reviewed in a state-of-the-art report *fib* bulletin [23]), and the reinforced solid method (RSM) [14], [15], [9]–[12], [18].

2.2. Idealization of material response

Limit analysis assumes that materials behave in a rigid-plastic manner. Since the material response is not perfectly plastic, equivalent reduced plastic strengths need to be defined for the application of the RSM:

Yielding conditions for concrete. The compressive strength of concrete f_c is considered with a reduced value to account for the material brittleness and effects of transversal strains. The tensile strength of concrete is neglected for equilibrium.

Yielding conditions for reinforcement. Reinforcing bars are assumed to be perfectly plastic, capable to resist only axial stresses. They are also assumed to be perfectly bonded to the concrete and distributed at such small intervals that the forces in them can be replaced by an equivalent stress distribution in the concrete. All these assumptions are allowed with basis on the lower bound theorem, once they will result in stresses in the reinforcement that are statically admissible. Kaufmann [20] contextualizes objectively the above-mentioned considerations: *Apart from the assumption of perfectly plastic reinforcement, these idealizations are quite crude. In a real structure, reinforcing bars are not infinitely thin, and considerable transverse shear may occur in reinforcement ("dowel action"). Bond stresses are limited by the bond strength, resulting in finite development lengths. The crack spacings are not infinitely small and tension stiffening effects occur. On the other hand, the analysis of a structure is simplified to a great extent by these assumptions, and their influence on the ultimate load is often negligible.*"

Yielding conditions for reinforced concrete. Until now, yielding conditions were set for each material individually and not for reinforced concrete, a heterogenous material. In the application of limit analysis methods to structural concrete, concrete and reinforcement are considered together as a continuum with resistance given by the linear combination of the resistances of the individual materials. Limit analysis may be applied to reinforced concrete if there is sufficient deformation capacity to develop the plastic stress redistribution required in the element.

2.3 RSM: the applied stresses

In the three-dimensional space, the stresses at a point referred to a rectangular coordinate system x, y and z are completely defined by the symmetrical stress tensor:

$$S = \begin{bmatrix} \sigma_x & \tau_{xy} & \tau_{xz} \\ \tau_{xy} & \sigma_y & \tau_{yz} \\ \tau_{xz} & \tau_{yz} & \sigma_z \end{bmatrix} \tag{1}$$

The positive sign convention for the six stress components is shown in Figure 4a: normal stresses σ_x, σ_y and σ_z are positive as tensile stresses; shear stresses τ_{xy} and τ_{xz} are positive in the coordinate directions in a section with the x-axis as an outwardly directed normal of the element face; shear stresses τ_{xy} and τ_{yz} are positive in the coordinate directions in a section with the y-axis as an outwardly directed normal of the element face; shear stresses τ_{xz} and τ_{yz} are positive in the coordinate directions in a section with the z-axis as an outwardly directed normal of the element face.
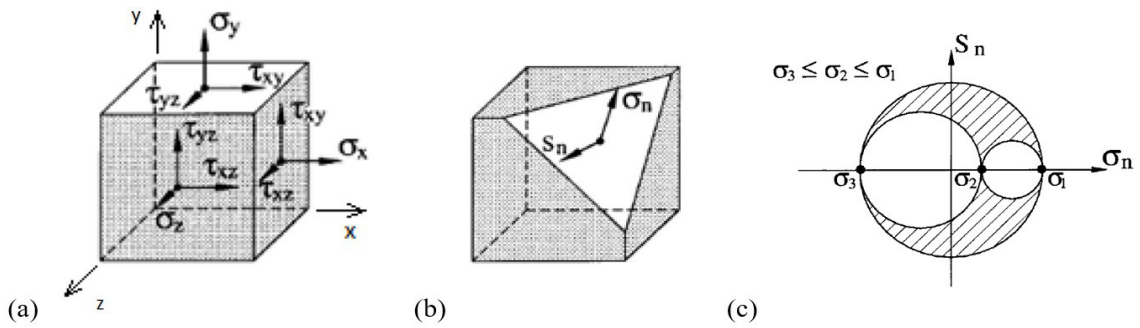
Figure 4. (a) Stress components in a solid element; (b) normal and shear stresses in an arbitrary plane; (c) Mohr circle for 3-D stresses in a point (adapted from Foster et al. [12])

For any oblique plane having a unit normal $\boldsymbol{n} = \{n_x, n_y, n_z\}$ passing through a point P, the stresses at point P can resolved into a component normal to the plane (σ_n) and a shear component parallel to the plane (S_n), as shown in Figure 4b. For a stress to be principal, $S_n = 0$ which implies that:

$$\begin{cases} \sigma_x n_x + \tau_{xy} n_y + \tau_{xz} n_z = \sigma_n n_x \\ \tau_{xy} n_x + \sigma_y n_y + \tau_{yz} n_z = \sigma_n n_y \\ \tau_{xz} n_x + \tau_{yz} n_y + \sigma_z n_z = \sigma_n n_z \end{cases} \tag{2}$$

As all three components of $\boldsymbol{n}$ cannot be zero, the solution is nontrivial only if the determinant of the coefficients $\backslash\sigma\backslash = 0$, that is:

$$\begin{vmatrix} \sigma_x - \sigma_n & \tau_{xy} & \tau_{xz} \\ \tau_{xy} & \sigma_y - \sigma_n & \tau_{yz} \\ \tau_{xz} & \tau_{yz} & \sigma_z - \sigma_n \end{vmatrix} = 0 \tag{3}$$

Expansion of the equation above leads to the characteristic equation:

$$\sigma_n^3 - I_1 \sigma_n^2 + I_2 \sigma_n - I_3 = 0 \tag{4}$$

where I_1, I_2 and I_3 are the invariants of the stress tensor given by:

$$\begin{aligned} I_1 &= \sigma_x + \sigma_y + \sigma_z = \sigma_1 + \sigma_2 + \sigma_3 \\ I_2 &= \sigma_x \sigma_y + \sigma_y \sigma_z + \sigma_x \sigma_z - \tau_{xy}^2 - \tau_{yz}^2 - \tau_{xz}^2 = \sigma_1 \sigma_2 + \sigma_2 \sigma_3 + \sigma_1 \sigma_3 \\ I_3 &= \sigma_x \sigma_y \sigma_z + 2\tau_{xy} \tau_{xz} \tau_{yz} - \sigma_x \tau_{yz}^2 - \sigma_y \tau_{xz}^2 - \sigma_z \tau_{xy}^2 = \sigma_1 \sigma_2 \sigma_3 \end{aligned} \tag{5}$$

where σ_1, σ_2 e σ_3 are the principal stresses, ordered such that $\sigma_3 \leq \sigma_2 \leq \sigma_1$. The principal stress directions $\boldsymbol{n}_i = \{n_{ix}, n_{iy}, n_{iz}\}$ (i = 1, 2, 3) are obtained from:

$$n_{ix} = -\frac{c_{iy}c_{iz}}{C_i}; \quad n_{iy} = -\frac{c_{ix}c_{iz}}{C_i}; \quad n_{ix} = -\frac{c_{ix}c_{iy}}{C_i} \tag{6}$$

where $C_i = \sqrt{c_{ix}^2\, c_{iy}^2 + c_{ix}^2\, c_{iz}^2 + c_{iy}^2\, c_{iz}^2}$ and

$$c_{ix} = \left(\sigma_x - \sigma_i\right)\tau_{yz} - \tau_{xy}\tau_{xz}; \quad c_{iy} = \left(\sigma_y - \sigma_i\right)\tau_{xz} - \tau_{xy}\tau_{yz}; \quad c_{iz} = \left(\sigma_z - \sigma_i\right)\tau_{xy} - \tau_{xz}\tau_{yz} \tag{7}$$

Once that the principal stresses have been found in magnitude and direction, the stresses on any oblique plane can be determined from:

$$\sigma_n = \sigma_1 n_1^2 + \sigma_2 n_2^2 + \sigma_3 n_3^2; \quad S_n^2 = \sigma_1^2 n_1^2 + \sigma_2^2 n_2^2 + \sigma_3^2 n_3^2 - \sigma_n^2 \tag{8}$$

where n_1, n_2, n_3 are the direction cosines relative to the principal axes of a vector normal to the plane. The point (σ_n, S_n) lies within the hatched region in Figure 4c. For the planes yz, xz and xy, the shear stresses are calculated, respectively, by:

$$S_x = \sqrt{\tau_{xy}^2 + \tau_{xz}^2}; \quad S_y = \sqrt{\tau_{xy}^2 + \tau_{yz}^2}; \quad S_z = \sqrt{\tau_{xz}^2 + \tau_{yz}^2} \tag{9}$$

Notes on shear stresses. There are eight combinations of signs for given absolute values of the shear stresses τ_{xy}, τ_{xz} and τ_{yz}, as shown in Table 1, that can be grouped into two subgroups. Let us consider a stress state with three positive shear stresses (sign combination #1). If the coordinate system is rotated 180^0 about the x-axis, the same shear stresses referred to the new coordinate system should be written with the sign combination #2; if the original coordinate system is rotated 180^0 about the y-axis, the shear stresses should be written with the sign combination #3; if, however, the original coordinate system is rotated 180^0 about the z-axis, shear stresses should be written with the sign combination #4. These transformations are represented in Figure 5, showing the physical equivalence between the so-called *positive shear stress Case 1*. Let us now consider a stress state with all three shear stresses being negative. Similarly, sign combinations #6 to #8 are physically equivalent to sign combination #5, and they all can be grouped into the so-called *negative shear stress Case 2*, as shown by the transformations in Figure 6.

Table 1. Shear stress sign combinations

Case 1	Sign combination			Case 2	Sign combination		
	τ_{xy}	τ_{xz}	τ_{yz}		τ_{xy}	τ_{xz}	τ_{yz}
# 1	+	+	+	# 5	-	-	-
# 2	-	-	+	# 6	+	+	-
# 3	-	+	-	# 7	+	-	+
# 4	+	-	+	# 8	-	+	+

Rev. IBRACON Estrut. Mater., vol. 16, no. 4, e16407, 2023

6/20

(a): (+,+,+)   (b): (-,-,+)   (c): (-,+,-)   (d): (+,-,-)

Figure 5. Positive shear stresses in Case 1

(a): (-,-,-)   (b): (+,+,-)   (c): (+,-,+)   (d): (-,+,+)
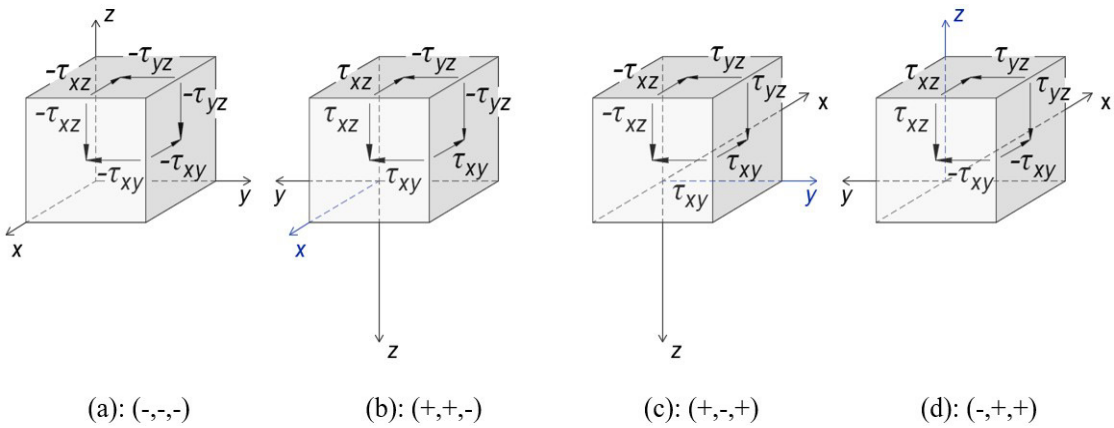
Figure 6. Negative shear stresses in case 2. Legend: (±, ±, ±) = (signal of τ_{xy}, signal of τ_{xz}, signal of τ_{yz})

2.4 RSM: the system of resistance

Let us consider a concrete cube with smeared reinforcement in the x-, y- and z-directions, delimited by an inclined plane corresponding to a crack, this plane being orthogonal to the larger principal stress (Figure 7). It is assumed that the crack face is crossed by the reinforcement in three directions but is free from any normal or shear stresses. The applied stresses (S) are resisted by equivalent stresses on concrete (S_c) and equivalent reinforcement stresses (S_s), as shown in Figure 8a:

$$S = S_c + S_s$$

$$\begin{bmatrix} \sigma_x & \tau_{xy} & \tau_{xz} \\ \tau_{yx} & \sigma_y & \tau_{yz} \\ \tau_{zx} & \tau_{zy} & \sigma_z \end{bmatrix} = \begin{bmatrix} \sigma_x - f_{tx} & \tau_{xy} & \tau_{xz} \\ \tau_{yx} & \sigma_y - f_{ty} & \tau_{yz} \\ \tau_{zx} & \tau_{zy} & \sigma_z - f_{tz} \end{bmatrix} + \begin{bmatrix} f_{tx} & 0 & 0 \\ 0 & f_{ty} & 0 \\ 0 & 0 & f_{tz} \end{bmatrix} \tag{10}$$

Concrete must resist both the difference between the normal applied stresses and the normal stresses carried by the reinforcement ($\sigma_{ci} = \sigma_i - f_{ti}$), and the three shear stress components (τ_{xy}, τ_{xz}, τ_{yz}); reinforcement, on the other hand, must resist the equivalent reinforcement stresses f_{tx}, f_{ty}, f_{tz} (reinforcement bar stresses distributed over the concrete area). It is assumed that reinforcing steel cannot carry shear stress.
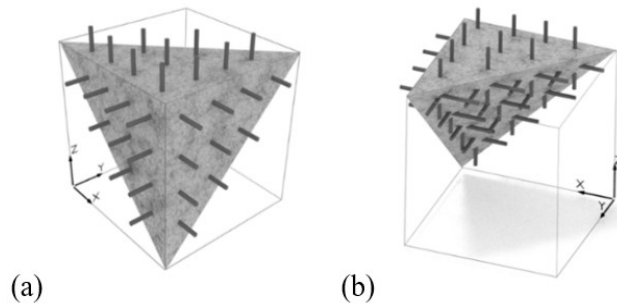
Figure 7. Cracked solid element with reinforcement in three orthogonal directions: (a) side view; (b) view of the inclined crack plane crossed by the reinforcement

The principal concrete stresses are derived from the concrete characteristic equation:

$$\sigma_n^3 - I_{c1}\sigma_n^2 + I_{c2}\sigma_n - I_{c3} = 0 \tag{11}$$

where the I_{c1}, I_{c2}, I_{c3} are the invariants of the concrete stress tensor:

$$
\begin{aligned}
I_{c1} &= \sigma_{cx} + \sigma_{cy} + \sigma_{cz} = \left(\sigma_x + \sigma_y + \sigma_z\right) - \left(f_{tx} + f_{ty} + f_{tz}\right) \\
I_{c2} &= \sigma_{cx}\sigma_{cy} + \sigma_{cy}\sigma_{cz} + \sigma_{cx}\sigma_{cz} - \tau_{xy}^2 - \tau_{yz}^2 - \tau_{xz}^2 \\
I_{c3} &= \sigma_{cx}\sigma_{cy}\sigma_{cz} + 2\tau_{xy}\tau_{xz}\tau_{yz} - \sigma_x\tau_{yz}^2 - \sigma_y\tau_{xz}^2 - \sigma_z\tau_{xy}^2
\end{aligned}
\tag{12}
$$

When one principal concrete stress is zero (σ_{c1}=0), the third invariant of the concrete stresses $I_{c3} = 0$, and the latter the characteristic equation reduces to:

$$\sigma^2 - I_{c1}\sigma + I_{c2} = 0 \tag{13}$$

which has the roots:

$$
\left.\begin{aligned}
\sigma_{c2} &= \sigma_{II} \\
\sigma_{c3} &= \sigma_{III}
\end{aligned}\right\} = \frac{1}{2}\left(I_{c1} \pm \sqrt{I_{c1}^2 - 4I_{c2}}\right)
\tag{14}
$$

The first term in Equation 14 defines the center of the 2 to 3 principal concrete stress circle and the second term, the radius. Figure 8b plots the Mohr´s circle for the applied stresses and, within the circles, the stress (σ_i, S_i), with $i = x$, y, z. They are resisted by equivalent concrete stresses (σ_{ci}, S_{ci}) and by equivalent steel stresses $f_{ti} = (\rho_{si} \times \sigma_{si})$, where ρ_{si} are the reinforcement ratios in the i-th directions, and σ_{si} are the equivalent steel stresses in the i-th directions.
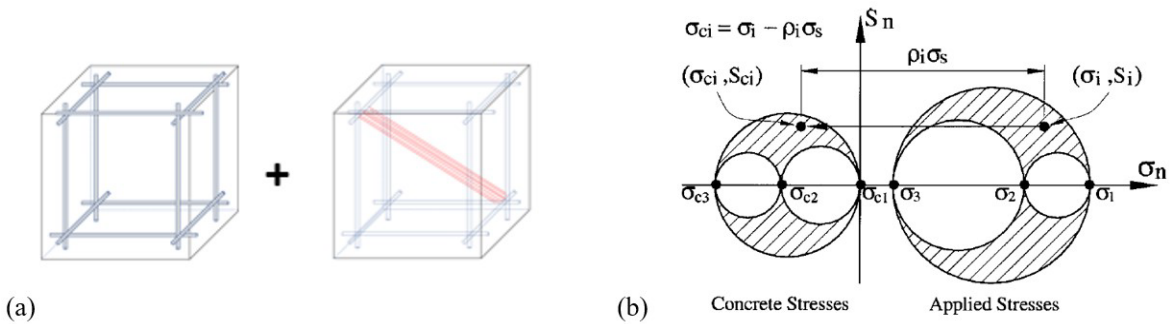
Figure 8. (a) System of resistance for a reinforced solid; (b) Mohr´s circle for the applied stresses and equivalent stresses on concrete and reinforcement [11]

2.5 RSM: equivalent stresses computation

From the eight combinations of signs of the three shear stresses, it is only necessary to consider two cases: all shear stresses positive or all shear stresses negative (or equivalently two shear stresses positive and one negative). This separation leads the ensuing formulation. For the complete deduction, please refer to Nielsen and Hoang [18].

2.5.1 Case 1a: positive shear stresses, reinforcement in three directions

Initially, the concrete normal stresses σ_{cx}, σ_{cy}, σ_{cz} are expressed as a function of the given shear stresses τ_{xy}, τ_{xz}, τ_{yz} and the Euler angles Ψ, θ, ϕ (angles used to describe the rotation for going from a rectangular coordinate x, y, z-system to the ξ, η, ζ-system when describing a stress state, as shown in Figure 9).

$$\sigma_{cx} = -\frac{\tau_{xy}\sin\psi\cos\theta + \tau_{xz}\sin\theta}{\cos\psi\cos\theta}; \ \sigma_{cy} = -\frac{\tau_{xy}\cos\psi\cos\theta + \tau_{yz}\sin\theta}{\sin\psi\cos\theta}; \ \sigma_{cz} = -\frac{\tau_{xz}\cos\psi\cos\theta + \tau_{yz}\sin\psi\cos\theta}{\sin\theta} \tag{15}$$

These formulas make possible to express the equivalent reinforcement stresses f_{tx}, f_{ty}, f_{tz} as:

$$f_{tx} = \sigma_x + \tau_{xy}\tan\psi + \tau_{xz}\frac{\tan\theta}{\cos\psi}; \ f_{ty} = \sigma_y + \tau_{xy}\frac{1}{\tan\psi} + \tau_{yz}\frac{\tan\theta}{\sin\psi}; \ f_{tz} = \sigma_z + \tau_{xz}\frac{\cos\psi}{\tan\theta} + \tau_{yz}\frac{\sin\psi}{\tan\theta} \tag{16}$$
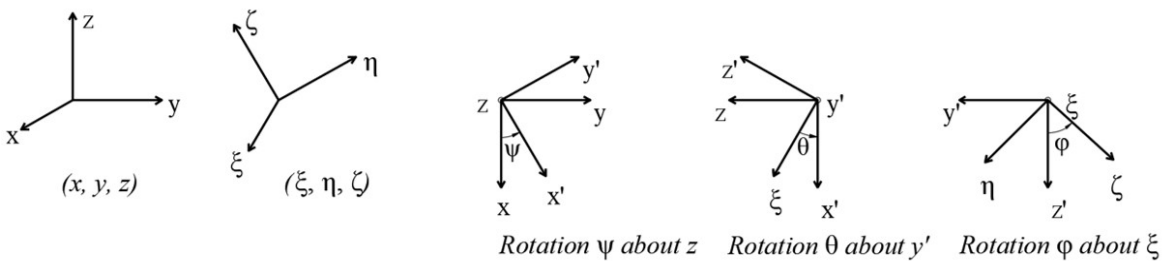
Figure 9. Euler angles

The total reinforcement consumption $R = f_{tx} + f_{ty} + f_{tz}$ is calculated by:

$$R = f_{tx} + f_{ty} + f_{tz} = \sigma_x + \sigma_y + \sigma_z + \tau_{xy}\left(\tan\psi + \frac{1}{\tan\psi}\right) + \tau_{xz}\left(\frac{\tan\theta}{\cos\psi} + \frac{\cos\psi}{\tan\theta}\right) + \tau_{yz}\left(\frac{\tan\theta}{\sin\psi} + \frac{\sin\psi}{\tan\theta}\right) \tag{17}$$

whose minimum is found for $\tan \psi = 1$ and $\tan \theta = \sqrt{2}/2$. Inserting these values into Equation 16, we find:

$$f_{tx} = \sigma_x + \left(\tau_{xy} + \tau_{xz}\right); \quad f_{ty} = \sigma_y + \left(\tau_{xy} + \tau_{yz}\right); \quad f_{tz} = \sigma_z + \left(\tau_{xz} + \tau_{yz}\right) \tag{18}$$

Concrete stresses are only dependent on the shear stresses:

$$\sigma_{cx} = \sigma_x - f_{tx} = -\left(\tau_{xy} + \tau_{xz}\right); \quad \sigma_{cy} = \sigma_y - f_{ty} = -\left(\tau_{xy} + \tau_{yz}\right); \quad \sigma_{cz} = \sigma_z - f_{tz} = -\left(\tau_{xz} + \tau_{yz}\right) \tag{19}$$

and the corresponding principal stresses are:

$$\left.\begin{array}{l} \sigma_{II} = \sigma_{c2} \\ \sigma_{III} = \sigma_{c3} \end{array}\right\} = -\left(\tau_{xy} + \tau_{xz} + \tau_{yz}\right) \mp \sqrt{\left(\tau_{xy} + \tau_{xz} + \tau_{yz}\right)^2 - 3\left(\tau_{xy}\tau_{xz} + \tau_{xz}\tau_{yz} + \tau_{yz}\tau_{xy}\right)} \tag{20}$$

2.5.2 Case 1b: positive shear stresses, reinforcement in two directions

i. If f_{tx} comes out negative in Equation 18, then:

$$f_{tx} = 0; \quad f_{ty} = \sigma_y + \tau_{yz} + \tau_{xy}\frac{\overbrace{\tau_{xy} + \tau_{xz}}^{>0}}{\left|\sigma_x\right|}; \quad f_{tz} = \sigma_z + \tau_{yz} + \tau_{xz}\frac{\overbrace{\tau_{xy} + \tau_{xz}}^{>0}}{\left|\sigma_x\right|} \tag{21}$$

ii. If f_{ty} comes out negative in Equation 18, then:

$$f_{tx} = \sigma_x + \tau_{xz} + \tau_{xy}\frac{\overbrace{\tau_{xy} + \tau_{yz}}^{>0}}{\left|\sigma_y\right|}; \quad f_{ty} = 0; \quad f_{tz} = \sigma_z + \tau_{xz} + \tau_{yz}\frac{\overbrace{\tau_{xy} + \tau_{yz}}^{>0}}{\left|\sigma_y\right|} \tag{22}$$

iii. If f_{tz} comes out negative in Equation 18, then:

$$f_{tx} = \sigma_x + \tau_{xy} + \tau_{xz}\frac{\overbrace{\tau_{xz} + \tau_{yz}}^{>0}}{\left|\sigma_z\right|}; \quad f_{ty} = \sigma_y + \tau_{xy} + \tau_{yz}\frac{\overbrace{\tau_{xz} + \tau_{yz}}^{>0}}{\left|\sigma_z\right|}; \quad f_{tz} = 0 \tag{23}$$

Concrete stresses are no longer only dependent on the shear stresses:

$$\sigma_{cx} = \sigma_x - f_{tx}; \quad \sigma_{cy} = \sigma_y - f_{ty}; \quad \sigma_{cz} = \sigma_z - f_{tz} \tag{24}$$

2.5.3 Case 1c: positive shear stresses, reinforcement in one direction

i. If f_{ty} comes out negative in Equation 21 or f_{tx} comes out negative in Equation 22:

Rev. IBRACON Estrut. Mater., vol. 16, no. 4, e16407, 2023

10/20

$$f_{tx} = 0; \quad f_{ty} = 0; \quad f_{tz} = \sigma_z + \frac{2\tau_{xy}\tau_{xz}\tau_{yz} - \sigma_x\tau_{yz}^2 - \sigma_y\tau_{xz}^2}{\sigma_x\sigma_y - \tau_{xy}^2} \tag{25}$$

ii.   If f_{tz} comes out negative in Equation 21 or f_{tx} comes out negative in Equation 23:

$$f_{tx} = 0; \quad f_{ty} = \sigma_y + \frac{2\tau_{xy}\tau_{xz}\tau_{yz} - \sigma_x\tau_{yz}^2 - \sigma_z\tau_{xy}^2}{\sigma_x\sigma_z - \tau_{xz}^2}; \quad f_{tz} = 0 \tag{26}$$

iii.   If f_{tz} comes out negative in Equation 22 or f_{ty} comes out negative in Equation 23:

$$f_{tx} = \sigma_x + \frac{2\tau_{xy}\tau_{xz}\tau_{yz} - \sigma_y\tau_{xz}^2 - \sigma_z\tau_{xy}^2}{\sigma_y\sigma_z - \tau_{yz}^2}; \quad f_{ty} = 0; \quad f_{tz} = 0 \tag{27}$$

Concrete stresses, once again, do not depend only on the shear stresses:

$$\sigma_{cx} = \sigma_x - f_{tx}; \; \sigma_{cy} = \sigma_y - f_{ty}; \; \sigma_{cz} = \sigma_z - f_{tz} \tag{28}$$

2.5.4 Case 1d: positive shear stresses, no reinforcement required

When f_{tx}, f_{ty} and f_{tz} all become negative in Equations 26 through 28, no reinforcement is required. This condition occurs when:

$$\sigma_x\sigma_y\sigma_z + 2\tau_{xy}\tau_{xz}\tau_{yz} - \sigma_x\tau_{yz}^2 - \sigma_y\tau_{xz}^2 - \sigma_z\tau_{xy}^2 < 0 \tag{29}$$

In this case, all principal stresses are negative (compressive).

2.3.5 Case 2a: negative shear stresses, biaxial concrete compression

The shear stresses with the larger absolute values are considered positive and the shear stress with the smaller absolute value is considered negative. Analyzing Equation 20 for the concrete principal stresses, biaxial compression (σ_{II} e $\sigma_{III} < 0$) occurs if:

$$\tau_{xy}\tau_{xz} + \tau_{xz}\tau_{yz} + \tau_{xy}\tau_{yz} > 0 \tag{30}$$

In this case, the formulas for Case 1 may be used when $|\tau_{yz}|$ is the smaller absolute shear stress. Otherwise, the designer should rename axes according to the following scheme:

If $|\tau_{xy}|$ is the smaller one: $x \rightarrow y \quad y \rightarrow z \quad z \rightarrow x$ \hfill (31)

If $|\tau_{xz}|$ is the smaller one: $x \rightarrow z \quad y \rightarrow x \quad z \rightarrow y$ \hfill (32)

Rev. IBRACON Estrut. Mater., vol. 16, no. 4, e16407, 2023

11/20

2.5.6 Case 2b: negative shear stresses, uniaxial concrete compression

Once again, the shear stresses with the larger absolute values are considered positive and the shear stress with the smaller absolute value is considered negative. Analyzing Equation 20 for the concrete principal stresses, uniaxial compression (only $\sigma_{III} < 0$) occurs when

$$\tau_{xy}\tau_{xz} + \tau_{xz}\tau_{yz} + \tau_{xy}\tau_{yz} < 0 \tag{33}$$

Considering that $|\tau_{yz}|$ is the smaller absolute shear stress, the equivalent reinforcement stresses are:

$$f_{tx} = \sigma_x - \frac{\tau_{xy}\tau_{xz}}{\tau_{yz}}; \ f_{ty} = \sigma_y - \frac{\tau_{xy}\tau_{yz}}{\tau_{xz}}; \ f_{tz} = \sigma_z - \frac{\tau_{xz}\tau_{yz}}{\tau_{xy}} \tag{34}$$

If f_{tx} turns out negative in Equation 34, Formula 21 from Case 1 is valid; if f_{ty} comes out negative in Equation 34, Formula 22 is valid; if, finally, f_{tz} comes out negative in Equation 34, Formula 23 is valid. One may continue using the formulas from Case 1, Equations 25 to 27 and 30, when further negative values appear. Concrete stresses are calculated by

$$\sigma_{cx} = \sigma_x - f_{tx} = \frac{\tau_{xy}\tau_{xz}}{\tau_{yz}}; \quad \sigma_{cy} = \sigma_y - f_{ty} = \frac{\tau_{xy}\tau_{yz}}{\tau_{xz}}; \quad \sigma_{cz} = \sigma_z - f_{tz} = \frac{\tau_{xz}\tau_{yz}}{\tau_{xy}} \tag{35}$$

Concrete principal stresses are

$$\sigma_{II} = 0; \quad \sigma_{III} = \sigma_{cx} + \sigma_{cy} + \sigma_{cz} = \underbrace{\frac{\tau_{xy}\tau_{xz}}{\tau_{yz}} + \frac{\tau_{xy}\tau_{yz}}{\tau_{xz}} + \frac{\tau_{xz}\tau_{yz}}{\tau_{xy}}}_{<0} \tag{36}$$

When $|\tau_{xy}|$ is the smaller shear stress, Formulas 34 to 36 for Case 2b may be applied when transformations in Equation 31 are applied. When $|\tau_{xz}|$ is the smaller one, the transformations (32) apply.

The design equations for cases 1a, 1b, 1c, 1d, 2a, and 2b are summarized in Table 2.

2.6 RSM: reinforcement design and concrete verification

Reinforcement is designed on the assumption of utilization of the bars up to the design value, and stresses must be limited to:

$$f_{tx} \le \rho_{sx} f_{yd}; \quad f_{ty} \le \rho_{sy} f_{yd}; \quad f_{tz} \le \rho_{sz} f_{yd} \tag{37}$$

where ρ_{sx}, ρ_{sy}, ρ_{sz} are the reinforcement ratio in the x-, y- and z-directions, respectively, and f_{yd} is the design value of the reinforcement steel yield stress.

Concrete stresses are required to satisfy:

$$-\sigma_{III} \le \nu f_{cd} \tag{38}$$

where f_{cd} is the design compression strength of concrete, and v is the efficiency factor introduced to account for both confinement effects, as in the case of concrete in biaxial or triaxial compression, disturbance effects such as caused by transmission of tension fields through compression fields, and micro-cracking in the concrete paste due to shrinkage. Then, v accounts for the imperfect assumption that concrete behaves as a rigid-plastic material and ensures that ductility demands are met. The following values of v are indicated by the *fib* Model Code [4]:

    i. If no reinforcement has yielded and at least one principal stress is in tension, then:

$$v = \frac{1,18}{1,14+0,00166\sigma_{si}} \leq 1 \tag{39}$$

where σ_{si} is the maximum tensile stress (in MPa) in any layer of the reinforcing steel

    ii. If one or more layers of reinforcement yield:

$$v = \left(1-0,032\left|\delta_i\right|\right)\frac{1,18}{1,14+0,00166f_{yd}} \tag{40}$$

where δ_i is given by Equation 42 ($i = x, y, z$).

    iii. If all principal stresses are compressive, v may be taken as 1,0 or determined in accordance with more elaborate expressions for the strength under multiaxial states of stress, such as the one given by Ottosen [4], [24]:

$$\alpha\frac{J_2}{f_{cm}^2} + \lambda\frac{\sqrt{J_2}}{f_{cm}} + \beta'\frac{I_1}{f_{cm}} - 1 = 0 \tag{41}$$

where I_1 and J_2 characterize the state of stress considered, and f_{cm} is the concrete uniaxial compressive strength.

In a solid subject to increasing loads, the stress field is continuously redistributed, starting from an initial approximately elastic state, followed by cracking of concrete, and yielding of steel. Through this process, elements shall be capable of allowing for sufficient plastic strains to prevent local rupture before the calculated stress distribution has been attained. Foster et al. [12] alert that "*designers must critically examine the load path being assumed to satisfy themselves that a sufficient level of ductility is available to meet the demands of the imposed tractions.*" For this purpose, they presented an expression for the enclosed angle between the principal direction of the applied stresses and those of the concrete stresses:

$$\delta_i \leq \cos^{-1}\left|n_{ix}n_{cix} + n_{iy}c_{ciy} + n_{iz}n_{ciz}\right| \tag{42}$$

where n_{ci} ($i = 1, 2, 3$) are the direction cosines of the concrete stress tensor, as shown in Figure 10. They suggested a limit of 25 degrees to δ_i, value that was later revised by the Model Code [4] to 15 degrees.
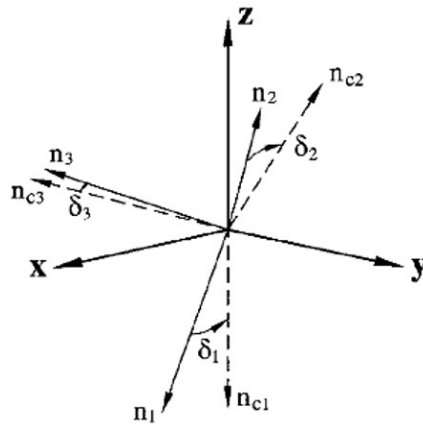
Figure 10. Comparison of concrete principal stress directions and the principal stress directions for the case of optimum reinforcement [12]

Table 2. Summary of design equations for individual elements

Reinf	Cases	f_{tx}	f_{ty}	f_{tz}	Condition
⊥	1a +++	$\sigma_x + (\tau_{xy} + \tau_{xz})$	$\sigma_y + (\tau_{xy} + \tau_{yz})$	$\sigma_z + (\tau_{xz} + \tau_{yz})$	$f_{tx}, f_{ty}, f_{tz} > 0$
''	2a ++-	$\sigma_x + (\tau_{xy} + \tau_{xz})$	$\sigma_y + (\tau_{xy} + \tau_{yz})$	$\sigma_z + (\tau_{xz} + \tau_{yz})$	$f_{tx}, f_{ty}, f_{tz} > 0$ $\tau_{xy}\tau_{xz} + \tau_{xz}\tau_{yz}$ $+ \tau_{xy}\tau_{yz} > 0$
''	2b ++-	$\sigma_x - \dfrac{\tau_{xy}\tau_{xz}}{\tau_{yz}}$	$\sigma_y - \dfrac{\tau_{xy}\tau_{yz}}{\tau_{xz}}$	$\sigma_z - \dfrac{\tau_{xz}\tau_{yz}}{\tau_{xy}}$	$f_{tx}, f_{ty}, f_{tz} > 0$ $\tau_{xy}\tau_{xz} + \tau_{xz}\tau_{yz}$ $+ \tau_{xy}\tau_{yz} < 0$
⊥	1b/ 2	$\sigma_x + \tau_{xy} - \tau_{xz}\dfrac{\tau_{xz} + \tau_{yz}}{\sigma_z}$	$\sigma_y + \tau_{xy} - \tau_{yz}\dfrac{\tau_{xz} + \tau_{yz}}{\sigma_z}$	0	$f_{tz} < 0$ $f_{tx}, f_{ty} > 0$
⊥	1b/ 2	$\sigma_x + \tau_{xz} - \tau_{xy}\dfrac{\tau_{xy} + \tau_{yz}}{\sigma_y}$	0	$\sigma_z + \tau_{xz} - \tau_{yz}\dfrac{(\tau_{xy} + \tau_{yz})}{\sigma_y}$	$f_{ty} < 0$ $f_{tx}, f_{tz} > 0$
⊥	1b/ 2	0	$\sigma_y + \tau_{yz} - \tau_{xy}\dfrac{\tau_{xy} + \tau_{xz}}{\sigma_x}$	$\sigma_z + \tau_{yz} - \tau_{xz}\dfrac{\tau_{xy} + \tau_{xz}}{\sigma_x}$	$f_{tx} < 0$ $f_{ty}, f_{tz} > 0$
⊥	1c/ 2	$\sigma_x + \dfrac{2\tau_{xy}\tau_{xz}\tau_{yz} - \sigma_y\tau_{xz}^2 - \sigma_z\tau_{xy}^2}{\sigma_y\sigma_z - \tau_{yz}^2}$	0	0	$f_{ty}, f_{tz} < 0$ $f_{tx} > 0$
⊥	1c/ 2	0	$\sigma_y + \dfrac{2\tau_{xy}\tau_{xz}\tau_{yz} - \sigma_x\tau_{yz}^2 - \sigma_z\tau_{xy}^2}{\sigma_x\sigma_z - \tau_{xz}^2}$	0	$f_{tx}, f_{tz} < 0$ $f_{ty} > 0$
⊥	1c/ 2	0	0	$\sigma_z + \dfrac{2\tau_{xy}\tau_{xz}\tau_{yz} - \sigma_x\tau_{yz}^2 - \sigma_y\tau_{xz}^2}{\sigma_x\sigma_y - \tau_{xy}^2}$	$f_{tx}, f_{ty} < 0$ $f_{tz} > 0$
⊥	1d/ 2	0	0	0	$\sigma_x\sigma_y\sigma_z + 2\tau_{xy}\tau_{xz}\tau_{yz}$ $-\sigma_x\tau_{yz}^2 - \sigma_y\tau_{xz}^2$ $-\sigma_z\tau_{xy}^2 < 0$

Notes:
(1) Sign convention: positive normal stress for tension.
(2) Case 1: (sign of τ_{xy}, sign of τ_{xz}, sign of τ_{yz}) = (+, +, +), (+, -, -), (-, +, -), (-, -, +) → consider $+|\tau_{xy}|$, $+|\tau_{xz}|$ and $+|\tau_{yz}|$
(3) Case 2: (sign of τ_{xy}, sign of τ_{xz}, sign of τ_{yz}) = (+, +, -), (+, -, +), (-, +, +), (-, -, -)
   → If $|\tau_{yz}|$ is the smallest absolute shear stress: consider $+|\tau_{xy}|$, $+|\tau_{xz}|$ and $-|\tau_{yz}|$.
   → If $|\tau_{xy}|$ is the smallest absolute shear stress: x→y, y→z, z→x . Consider: $+|\tau_{xy}|$, $+|\tau_{xz}|$ and $-|\tau_{yz}|$. Calculate reinf. and retrieve original axes.
   → If $|\tau_{xz}|$ is the smallest absolute shear stress: x→z, y→x, z→y . Consider $+|\tau_{xy}|$, $+|\tau_{xz}|$ and $-|\tau_{yz}|$. Calculate reinf. and retrieve original axes.
(4) Concrete stresses (all cases): $\sigma_{cx} = \sigma_x - f_{tx}$; $\sigma_{cy} = \sigma_y - f_{ty}$; $\sigma_{cz} = \sigma_z - f_{tz}$. Concrete verification as described in section 2.5.
(5) Reinforcement: $\rho_{sx} = f_{tx} / f_y$; $\rho_{sy} = f_{ty} / f_y$; $\rho_{sz} = f_{tz} / f_y$; and $a_s = \rho_s . A_c$

3 METHODOLOGY FOR THE DESIGN OF A STRUCTURAL MEMBER

As an example of the herein proposed methodology, the design of a reinforced concrete member by the RSM was performed according to the steps 1 to 3 described below:

Step 1: Linear analysis. An initial linear analysis was performed with the software *STRAP* version 12.5 from *Atir Engineering Software Development Ltd.* [25]. The structure was modeled with finite solid elements assuming uncracked material, linear stress-strain relationships, and the mean value of the concrete modulus of elasticity. From this initial model two output *.lst* files were obtained: one containing the geometry definition (nodal coordinates and element nodal incidence), and the other containing the complete stress field deriving from the analysis (nodal stresses).

Step 2: Data processing – individual element RSM design. An application was developed with Java programming language for data treatment using *Java Development Kit JDK 17*. This application was built to: (i) read the data from the *.lst* files created in step 1; (ii) treat the data, computing stress invariants, principal stresses and directions, and equivalent resisting stresses in each model node (both reinforcement stresses f_{tx}, f_{ty}, f_{tz} and concrete stresses); (iii) automatically assemble the calculated quantities into a *.vtk* file to be later accessed by a post processor. The flowchart of the application structure is presented in Figure 11.

Step3: Data analysis and structural member RSM design. The *.vtk* file was loaded into the software *Paraview* version 5.9.1 from *Kitware Inc.* This software, described by Ahrens et al. [26], is an open-source software system for 3D computer graphics, modeling, volume rendering and information visualization by operations such as clipping, slicing, filtering, or generating contours from the loaded data. At this point, a thorough analysis of the reinforcement requirements and concrete stresses sufficed for the global structural design and subsequent detailing by delimitation of zones with constant reinforcement ratio.

The methodology was applied to the RSM design of a structural component: a pile cap with dimension 1,90 m x 1,90 m, 0,80 m depth, concrete C30, supported by four rectangular 0,30 m x 0,30 m piles, subjected to a design load of P_d = 1 380 kN acting on the top of a 0,30 m x 0,80 m rectangular column. Though less usual in design practice, rectangular piles were chosen to facilitate modelling and visualization. For step 1, the definition of a 0,10 m mesh size led to a structural model with 3 400 cubic solid elements, as shown in Figure 12.
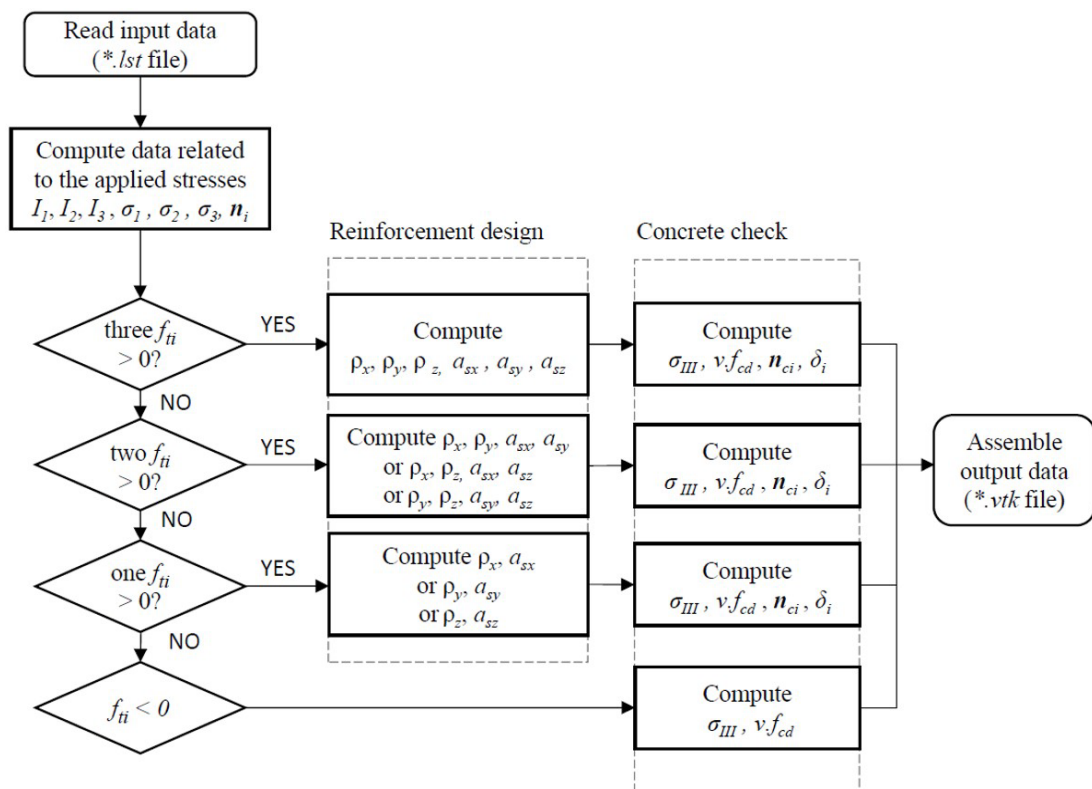
Figure 11. Flowchart of the developed application
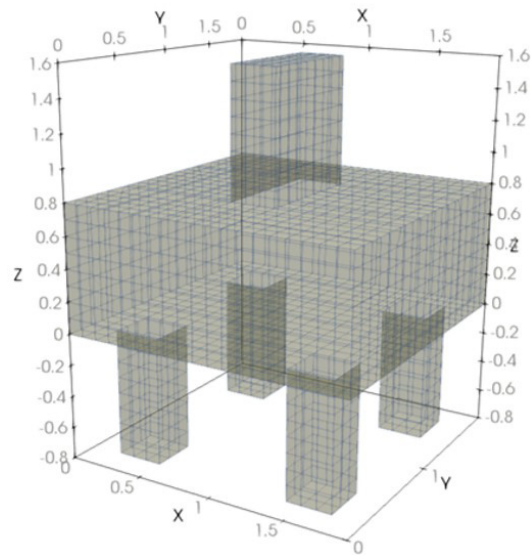
Figure 12. Structural solid model of a four-pile cap for the step 1 of the methodology

4 RESULTS AND DISCUSSIONS

4.1 Results for the four-pile cap designed by the RSM

The distribution of equivalent reinforcement stresses in the *x*- and *y*-directions, in cross sections passing through the center of gravity of the cap, are illustrated in Figure 13a and b, respectively. It should be noted that, according to the design, it was necessary to distribute reinforcement in the two lower thirds of the cap depth. It was proposed to reinforce the lower 0,25 m of the cap depth with reinforcement ratio $\rho_x = \rho_y = 0,5 \cdot (1,8+0,9)/435 = 0,31\%$, and the intermediate 0,25 m of the cap depth with $\rho_x = \rho_y = 0,5 \cdot (0,9+0)/435 = 0,10\%$. Doing so, the smeared total horizontal reinforcement amounted to $A_{sx} = A_{sy} = 19,5$ cm². Equivalent reinforcement stresses were also detected in the z-direction, as shown in Figure 14a, mainly at the regions highlighted by the red color, which corresponded to the intersection between the mid-depth plane and the compression struts. The maximum f_{tz} value was equal to 0,79 MPa and indicated the necessity of z-reinforcement at a ratio of $\rho_z = 0,79/435 = 0,18\%$. The largest equivalent concrete principal stresses were clearly distributed following the direction of the compressive struts, as shown in Figure 14b, where the solid elements with $\sigma_{c3} = \sigma_{III} < -1,0$ MPa were filtered.

(a)   (b)
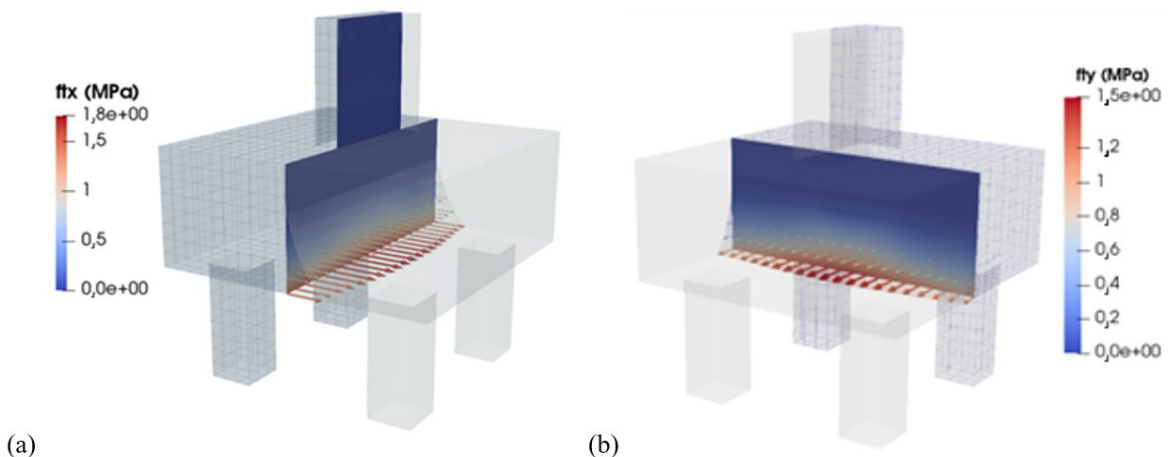
Figure 13. Four-pile cap analysis: reinforcement equivalent stresses (a) f_{tx} and (b) f_{ty}

Rev. IBRACON Estrut. Mater., vol. 16, no. 4, e16407, 2023

16/20

(a)   (b)
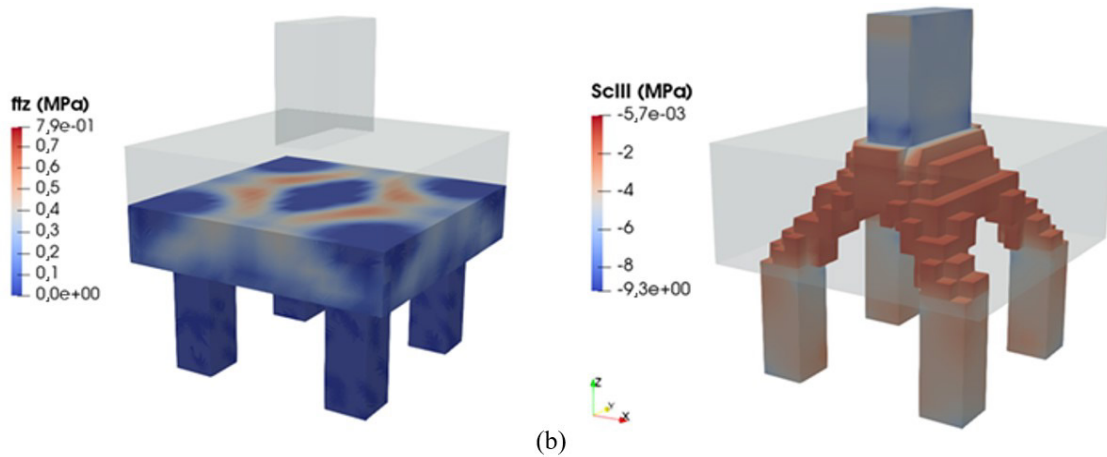
Figure 14. Four-pile cap: (a) reinforcement equivalent stress f_{tz}; (b) elements with concrete principal stress σ_{III} lower than -1,0 MPa

4.2 Validation of the RSM

Numerical simulations of the four-pile cap were performed using the software *ATENA 3D* version 5.9.0 from Červenka Consulting [27] to validate the design achieved for the four-pile cap. A fracture-plastic material model based on the classical orthotropic smeared crack formulation (CC3NonLinCementitious2) was assigned to the concrete elements; reinforcement was modeled either by discrete or smeared bars, considering bilinear stress-strain law for steel, with maximum strain limited to 10‰. The partial factor method (as prescribed in the *fib* Model Code [4] and in *Guidelines for Nonlinear Finite Element Analysis of Concrete Structures* [28]) was selected as the safety format for the non-linear analyses, meaning that design values were assigned to the basis variables. The arc-length solution method was selected as the solution scheme.

Five models were tested up to failure, two of which designed by the Strut and Tie Method (STM), and the other three designed by the Reinforced Solid Model (RSM). Model ⑤ was elaborated considering the discrete reinforcement designed by the STM; initially, we considered neglecting the concrete tensile strength just as it is done in the STM. However, for convergence purposes, a reduced f_{ctd} was set for concrete: $f_{ctd, reduced} = 0,10$ MPa $\approx 0,07 f_{ctd}$. The ultimate load for this model, just 2% higher the design load ($P_d = 1\,412$ kN), indicates the proper calibration of both material models and solution method chosen for the simulations. Model ③ was built with smeared reinforcement in three directions designed by the RSM, while in model ④ reinforcement in the z-direction was suppressed. Both models considered the reduced tensile strength so that a direct comparison could be established between the RSM and the STM results. The ultimate loads obtained by the simulations were, respectively, 1,54 x P_d and 1,46 x P_d. Model ① was built with smeared reinforcement designed by the RSM (see Figure 15a), and model ② with discrete reinforcement designed by the STM. Both considered $f_{ctd} = 1,46$ MPa as input value. The ultimate loads obtained by the simulations were, respectively, 1,78 P_d and 1,52 P_d. Figure 15b and Figure 16 plot the reinforcement stresses for the last step of the nonlinear analyses, where the x-reinforcement yielded with 10‰ strain. The load displacement curves for all performed numerical simulations are presented in Figure 17.

(a)   (b)
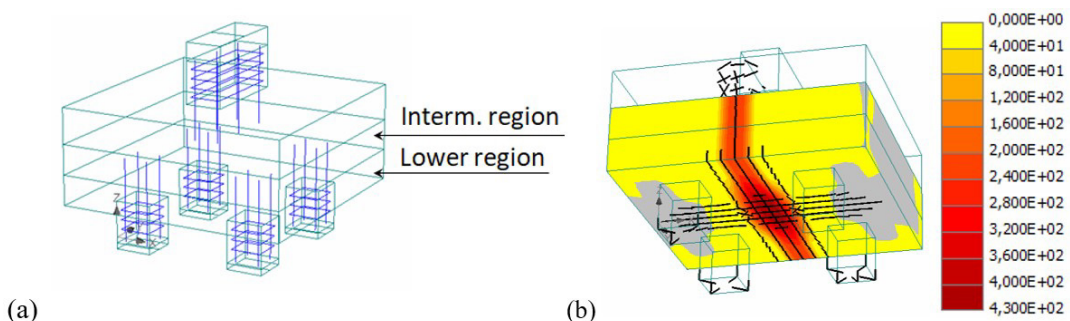
Figure 15. Numerical model ①: (a) reinforcement zones; (b) x-reinf. stresses (MPa) with crack pattern (crack widths > 0,1 mm only)
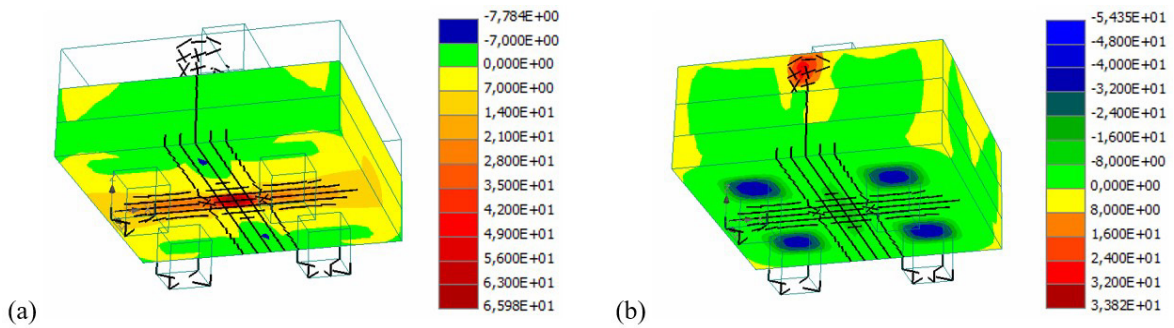
Figure 16. Numerical model ①: (a) y-reinf. stresses (MPa); (b) z-reinf. stresses (MPa)
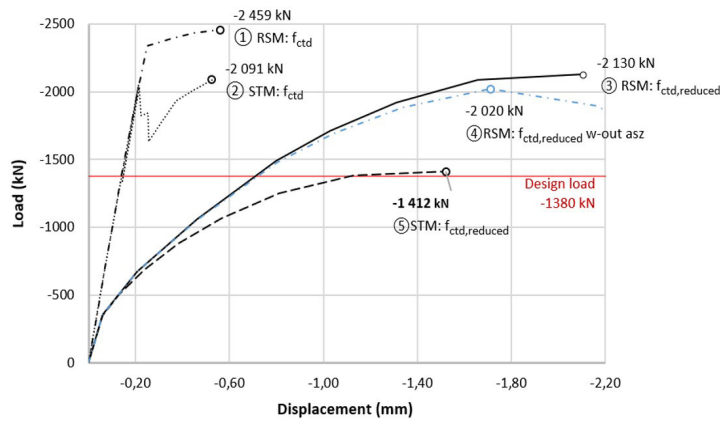
Figure 17. Load displacement curves for the performed numerical simulations

4.3 Discussion

The methodology presented for the RSM was applied to the design of a simple structural component to confirm the applicability of the proposed design method and to facilitate the discussion on the design variables.

Four-pile cap. The total required horizontal reinforcement for the RSM design was $A_{sx} = A_{sy} = 19,5$ cm^2, higher than the required reinforcement for a STM design ($A_{sx} = A_{sy} = 12,0$ cm^2) in which reinforcement in the x- and y-directions were all arranged at the bottom of the cap, maximizing the internal lever arm between tie and compression zone. The numerical simulations of models ③ and ④ indicated that reinforcement in the z-direction had little influence on the pile-cap collapse load, and this could be accounted on plastic redistribution of the equivalent reinforcement stresses in the z-direction. The pile cap could certainly be designed according to other well-established solutions. Brazilian design code [3] even explicitly recommends that the reinforcement be concentrated over the top of the piles when designing pile caps. However, the proposed application of methodology not only presents an alternative safe solution, but, more importantly, illustrates a procedure whose application may be efficiently extended to very complex structures.

Benefits of the method. Four main aspects are herein highlighted on behalf of the RSM for the design of structures with solid elements. First, the method predicates that all the structure volume participates in the resisting scheme, differently from the STM or the SFM, where stress fields are developed quantitatively in a few elements, and stress-free zones are disregarded outside the strut/tie zones. Second, the method relies neither on the development of a strut-and-tie scheme (or combined strut-and-tie schemes), nor on the definition of nodal geometries, nor on the application of an iterative procedure for the adjustment of the truss internal arms. Third, the method is applicable to the design or assessment of structural elements with general geometry, from the simplest to the most complex, subjected to any loading condition, even in discontinuity regions. Last, the RSM does not require running nonlinear analyses as in the application of strength reduction numerical methods. Examples of these methods are those presented by Mergny et al. [29], Abra and Ftima [30], and Yun et al. [31], which allow for the degradation of concrete by gradually reducing its tensile strength during the analysis in an iterative finite element analysis framework. The RSM is yet believed to be an efficient alternative in engineering practice due to its non-iterative application.

Rev. IBRACON Estrut. Mater., vol. 16, no. 4, e16407, 2023

18/20

Reinforcement layout. The application of the RSM provides the designer a field of required reinforcement throughout the structural volume, expressed in terms of a reinforcement ratio distribution. In this way, opposed to STM, where the reinforcement layout is often concentrated, the RSM leads to a distributed reinforcement layout.

Plasticity. In the RSM design, since the final resisting model follows the elastic solution element by element, and reinforcement is provided throughout the structure volume, less stress redistribution and less plastic deformation are expected than in the STM design. Consequently, a more distributed crack pattern and smaller crack widths are also expected, improving the structural performance in both Ultimate and Serviceability Limit States.

Design practice. Structural models in current design practice are predominantly composed of bar and shell elements, while the use of solid elements is still largely ignored. This condition may be ascribed to two main reasons: difficulties arisen in treating the large amount of data resulting from the finite element linear analysis and, probably, the lack of knowledge of the rules for proportioning the required reinforcement. This paper disclosures the established design rules and presents an example of an effective design tool for the application of the RSM. Finally, it is worth noting that a paragraph of the Model Code [5] entitled "3D Solids" is dedicated to this design method. Further studies of this subject, including those accounting on serviceability states and detailing aspects, though still missing in recent references, shall enhance its application.

5 CONCLUSIONS

The following conclusions have been derived from this research:

- The RSM for the ULS design of structures is justified by the static method, based on the lower bound theorem of the Limit Analysis of the Theory of Plasticity, and yields safe solutions. It can be applied to any kind of structure, from the simplest to those with complex geometry and loading conditions, including discontinuity regions.
- There is a full set of equations for the *reinforcement design* and *concrete verification* of individual solid elements from three-dimensional stress fields obtained from linear analyses. Any applied stress state can be resisted by equivalent stresses in the concrete and in the reinforcement distributed in up to three orthogonal directions.
- A computational routine was developed for the automatic design of all set of individual elements within a structural model.
- The utilization of a post processor for the visualization of the resistance system (i.e., concrete and reinforcement equivalent stresses) provided a clear understanding of both overall structural behavior and local effects.
- Verifications assisted by numerical simulations confirmed the safety of the Reinforced Solid Method, as expected. In the case of the analyzed four-pile cap, the design resistance resulted approximately 50% higher than the design load.

ACKNOWLEDGEMENTS

REFERENCES

[1] DIANAFEA. "Clinker silo." https://dianafea.com/project-clinkersilo (accessed May 1, 2022).

[2] W. Commons. "Hydroelectric dam animation." https://commons.wikimedia.org/wiki/File:Hydroelectric_dam_animation_esp.ogv (accessed May 1, 2022).

[3] Associação Brasileira de Normas Técnicas, *Projeto de Estruturas de Concreto: Procedimento*, NBR-6118, 2014.

[4] International Federations for Structural Concrete, *fib Model Code for Concrete Structures 2010.* Berlin: Ernst & Sohn, 2013.

[5] ACI Committee 318, *Building Code Requirements for Structural Concrete.* Detroit: Am. Concr. Inst., 2019.

[6] A. Boer, "Design strategy structural concrete in 3D: focusing on uniform forces results and sequential analysis," Ph.D. dissertation," Tech. Univ. Delft, Delft, 2010.

[7] A. P. Dolgikh and A. Podvysotskii, "A. Strength analysis of massive reinforced concrete structures using the method of equivalent shells," *Power Technol. Eng.*, vol. 44, no. 5, pp. 1, 2011.

[8] S. Lisichkin, "Safety enhancement in large hydraulic structures from new spatial reinforcement methods," *Hydrotechnical Constr.*, vol. 35, no. 3, pp. 116–123, 2001.

[9] S. B. Smirnov, "Problems of calculating the strength of massive concrete and reinforced concrete elements of complex hydraulic structures," *Power Technol. Eng.*, vol. 17, no. 9, pp. 471–476, 1983.

[10] Y. Kamezawa, N. Hayashi, I. Iwasaki, and M. Tada, "A study on design methods of RC structures based on FEM analysis," *Proc. Jpn. Soc. Civ. Eng.*, vol. 25, no. 502, pp. 103–122, Nov 1994. [in Japanese].

[11] P. Marti, N. Mojsilović, and S. J. Foster, "Dimensioning of orthogonally reinforced concrete solids," in *Struct. Concr. Switzerland, fib-CH, fib-Congr.*, Osaka, Japan, 2002, pp. 18–23.

[12] S. J. Foster, P. Marti, and N. Mojsilović, "Design of reinforcement concrete solids using stress analysis," *ACI Struct. J.*, vol. 100, pp. 758–764, 2003.

[13] International Federations for Structural Concrete, *Practioners's Guide to Finite Element Modelling of Reinforced Concrete Structures, State-of-Art Report* (*fib* Bulletin 45). Lausanne: *fib*, 2008.

[14] P. C. J. Hoogenboom and A. Boer, "Computation of reinforcement for solid concrete," *Heron*, vol. 53, no. 4, pp. 247–271, 2008.

[15] P. C. J. Hoogenboom and A. Boer, "Computation of optimal concrete reinforcement in three dimensions," in *Computational Modelling of Concrete Structures*, N. Bicanic, R. De Borst, H. Mang and G. Meschke, Eds., London: Taylor & Francis, 2010, pp. 639–646.

[16] R. K. L. Su, L. W. Yan, C. W. Law, J. L. Huang, and Y. M. Cheng, "The provision of reinforcement in concrete solids using the generalized genetic algorithm," *J. Comput. Civ. Eng.*, vol. 25, no. 3, pp. 211–217, Jan 2010.

[17] A. S. Zalesov, O. D. Rubin, and S. E. Lisichkin, "Higher safety of massive hydraulic structures based on improved design norms," *Hydrotechnical Constr.*, vol. 28, no. 9, pp. 554–558, 1994.

[18] M. P. Nielsen and L. C. Hoang, *Limit Analysis and Concrete Plasticity*, 3rd ed. Boca Raton: CRC Press, 2011.

[19] A. Muttoni, J. Schwartz, and B. Thürlimann, *Design of Concrete Structures with Stress Fields.* Basel: Birkhäuser, 1996.

[20] W. Kaufmann, "Strength and deformations of structural concrete subjected to in-plane shear and normal forces," Ph.D. dissertation," Inst. Struct. Eng., Swiss Fed. Inst. Technol., Zurich, 1998.

[21] K. P. Larsen, "Numerical limit analysis of reinforced concrete structures: computational modeling with finite elements for lower bound limit analysis of reinforced concrete structures," Ph.D. dissertation," Tech. Univ. Denmark, Denmark, 2010.

[22] W. Kaufmann and J. Mata-Falcón, "Structural concrete design in the 21st century: are limit analysis methods obsolete?," in *24th Czech Concr. Days*, Litomyšl, 2017.

[23] International Federations for Structural Concrete, *fib Bulletin 100, Design and Assessment with Strut-and-Tie Models and Stress Fields: from Simple Calculations to Detailed Numerical Analysis – State-of-the-Art Report*. Lausanne: *fib*, Sep. 2021.

[24] N. S. Ottosen, "A failure criterion for concrete," *J. Eng. Mech. Div.*, vol. 103, pp. 527–534, 1977.

[25] ATIR, *STRAP Structural Analysis Programs – User´s Manual.* Israel: ATIR Eng. Software Dev., Dec. 2005.

[26] J. Ahrens, B. Geveci, and C. Law, "ParaView: an end-user tool for large data visualization" in *Visualization Handbook*, C. D. Hansen and C. R. Johnson, Eds., Paises Bajos: Elsevier, 2005.

[27] V. Cervenka, L. Jendele, and J. Cervenka, *ATENA Program Documentation – Part 1: Theoryi.* Prague: Červenka Consulting Ltd., 2005.

[28] M. Hendriks, A. Boer, and B. Belletti, *Guidelines for Nonlinear Finite Element Analysis of Concrete Structures*. Netherlands: Rijkswaterstaat Centre Infrastruct., 2016.

[29] E. Mergny, M. Ansriou, A. Lespagnard, A. Ouaar, and P. Latteur, "Stress analysis for the reinforcement of concrete massive structures, compatible with building methods," in *Proc. Int. Assoc. Shell Spatial Struct (IASS) Symp 2015*, Amsterdam, 2015.

[30] O. Abra and M. Ben Ftima, "Strength reduction design method for reinforced concrete structures: generalization," *Eng. Struct.*, vol. 258, pp. 114134, Mar 2022.

[31] Y. M. Yun, H. Chae, and J. A. Ramirez, "A three-dimensional strut-and-tie model for a four-pile reinforced concrete cap," *J. Adv. Concr. Technol.*, vol. 17, no. 7, pp. 365–380, Jul 2019.